

A CHANDRA DEEP X-RAY EXPOSURE ON THE GALACTIC PLANE AND NEAR INFRARED IDENTIFICATION

K. Ebisawa, A. Paizis, T. J.-L. Couvoisier, P. Dubath¹, M. Tsujimoto², K. Hamaguchi, V. Beckmann³, A. Bamba, A. Senda, M. Ueno⁴, H. Kaneda, Y. Maeda, G. Sato⁵, S. Yamauchi⁶, R. Cutri⁷, and E. Nishihara⁸

¹INTEGRAL Science Data Centre, Chemin d'Écogia 16, 1290 Versoix, Switzerland

²Department of Astronomy and Astrophysics, Pennsylvania State University, University Park, PA 16802, USA

³Laboratory for High Energy Astrophysics, NASA/GSFC, Greenbelt, MD 20771, USA

⁴Department of Physics, Kyoto University, Kitashirakawa Oiwake-cho, Sakyo-ku, Kyoto, 606-8502, Japan

⁵Institute of Space and Astronautical Science, Yoshinodai, Sagami-hara, Kanagawa, 229-8510 Japan

⁶Faculty of Humanities and Social Sciences, Iwate University, Iwate, 020-8550, Japan

⁷IPAC, California Institute of Technology, code 100-22, 770 South Wilson Avenue, Pasadena, CA 91125, USA

⁸Gunma Astronomical Observatory, Nakayama Takayama-mura, Agatsuma-gun Gunma, 377-0702, Japan

ABSTRACT

Using the *Chandra* ACIS-I instruments, we have carried out a deep X-ray observation on the Galactic plane region at $(l, b) \approx (28.^\circ 5, 0.^\circ 0)$, where no discrete X-ray sources have been known previously. We have detected, as well as strong diffuse emission, 274 new point X-ray sources (4σ confidence) within two partially overlapping fields (~ 250 arcmin² in total) down to the flux limit $\sim 3 \times 10^{-15}$ erg s⁻¹ cm⁻² (2 – 10 keV) and $\sim 7 \times 10^{-16}$ erg s⁻¹ cm⁻² (0.5 – 2 keV). We clearly resolved point sources and the Galactic diffuse emission, and found that $\sim 90\%$ of the flux observed in our field of view originates from diffuse emission. Many point sources are detected *either* in the soft X-ray band (below 2 keV) or in the hard band (above 2 keV), and only a small number of sources are detected in both energy bands. On the other hand, most soft X-ray sources are considered to be nearby X-ray active stars. We have carried out a follow-up near-infrared (NIR) observation using SOFI at ESO/NTT. Most of the soft X-ray sources were identified, whereas only a small number of hard X-ray sources had counterparts in NIR. Using both X-ray and NIR information, we can efficiently classify the point X-ray sources detected in the Galactic plane. We conclude that most of the hard X-ray sources are background Active Galactic Nuclei seen through the Milky Way, whereas majority of the soft X-ray sources are nearby X-ray active stars.

Key words: Chandra; Milky way; ESO/NTT; Near-infrared; survey; diffuse emission.

1. CHANDRA OBSERVATION AND RESULTS

We have carried out two 100 ksec pointings with *Chandra* ACIS-I in AO1 (February 25 and 26, 2000) and AO2 (May 20, 2001), with slightly overlapping fields (Fig. 1). Total area of the observed field is ~ 250 arcmin². The first results from the AO1 observation has been published in Ebisawa et al. (2001). Detailed analysis of the new supernova remnant candidate in the field of view, AX J1843.8–0352/G28.6–0.1 (marked in Fig.), is reported in Ueno et al. (2003). The full results including the X-ray source catalog will be published in Ebisawa et al. (2004).

We have extracted an energy spectrum from our *Chandra* Galactic plane field (Fig. 2) by subtracting the instrumental background and excluding the AX J 1843.8–0352/G28.6–0.1 region (marked in Fig. 1). We found that the diffuse emission contributes to $\sim 90\%$ of the flux in the field of view, and that emission lines from highly ionized heavy elements are associated with the diffuse emission. This indicates that the Galactic ridge X-ray emission is truly diffuse, and its origin is probably a highly ionized plasma.

We have made $\log N - \log S$ curves in 2 – 10 keV and 0.5 – 2 keV from the surface density of the detected point sources (Fig. 3). Our results are also compared with those from the high Galactic region and Galactic center.

In the 2 – 10 keV band, after taking into account the Galactic absorption, our $\log N - \log S$ curve does not indicate significant excess over the extragalactic one. This indicates that most of the hard X-ray point sources we detected in the Galactic plane are in fact of extragalactic origin, presumably background

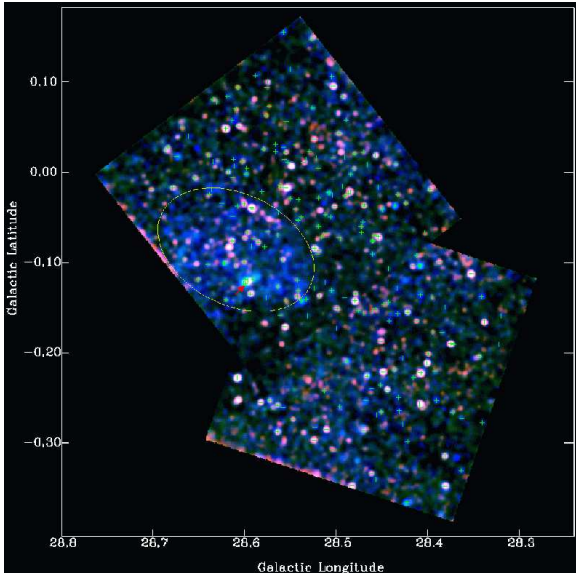


Figure 1. Superimposed image of the two Chandra observations (exposure and vignetting are corrected) in Galactic coordinates. South is AO1 and North is the AO2 field, each for 100 ksec exposure. This is a pseudo-color image such that soft X-rays in 0.5 – 2 keV, medium X-rays in 2 – 4 keV and hard hard X-rays in 4 – 8 keV are represented in red, green and blue, respectively (in the electronic version). The image is adaptively smoothed so that both the point sources and the diffuse emission are clearly visible. The 274 detected point source are marked with crosses. The region including the supernova remnant AX J 1843.8–0352/G28.6–0.1 (Bamba et al. 2001; Ueno et al. 2003) is shown with the yellow ellipse, within which an extended thermal blob named CXO J184357-35441 (Ueno et al. 2003) is marked with the red arrow. Note that the supernova remnant AX J 1843.8–0352/G28.6–0.1 is prominent in hard X-rays (“bluish” in this representation).

AGNs. If we compare the hard X-ray $\log N - \log S$ curve at the Galactic center region and that of the Galactic plane (Fig. 3, left), we see clear excess of the Galactic X-ray sources in the Galactic center region over the Galactic plane. In the soft X-ray band, on the other hand, contribution from the extragalactic sources is negligible since they are almost fully absorbed. Thus almost all the soft X-ray sources discovered in our Galactic plane field are considered to be Galactic.

2. NEAR INFRARED OBSERVATION AT ESO USING NTT/SOFI

Because of the heavy Galactic absorption, the near infrared band has a great advantage over the optical to identify dim X-ray sources in the Galactic plane. In order to identify X-ray point sources in our Chandra field, we have carried out a NIR follow-up observation at European Southern Observatory (ESO) using the New Technology Telescope with the SOFI

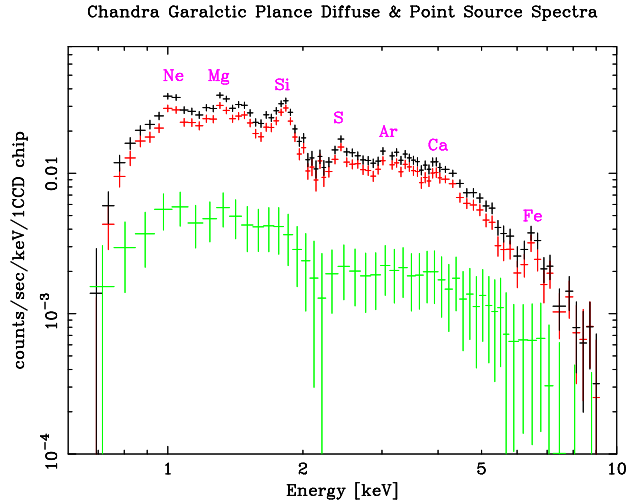


Figure 2. X-ray energy spectrum of our Chandra Galactic plane field. The AX J 1843.8–0352/G28.6–0.1 region (marked in Fig. 1) was excluded. Black (top) is the total emission in the field of view, and green (bottom) is the sum of the point sources, red (slightly lower than the black) is the residual diffuse emission.

infrared camera. The observations were carried out on the nights of July 28 and 29, 2002.

In Fig. 4, we plot angular distance between the Chandra point sources (classified with X-ray colors) and the nearest NIR sources detected by SOFI. If the separation between the Chandra source and SOFI source is less than $\sim 1.0''$, we identify the two sources. We can see that most of the soft X-ray sources (marked in red) have NIR counterparts, while only a small portion of the hard X-ray sources is identified in the NIR. This is consistent with the result from the $\log N - \log S$ analysis that most hard X-ray sources are extragalactic, whereas almost all the soft X-ray sources are Galactic.

3. CLASSIFICATION OF THE POINT SOURCES

Using both X-ray and NIR information, we may effectively classify X-ray point sources.

In Fig. 5, we show a histogram of the X-ray hardness ratio distribution and the intensity-hardness diagram. From the left panel in Fig. 5, we can see that the softest sources are most numerous, and most of them have NIR counterparts. With increasing hardness ratio, the number of sources first decreases, but again increases toward the hardest values. This clearly indicates the dichotomy of the point source population, Galactic population and extragalactic one.

In the right panel of Fig. 5, we can see that all the bright soft sources have NIR counterparts. Only several dim soft sources do not have counterparts, pre-

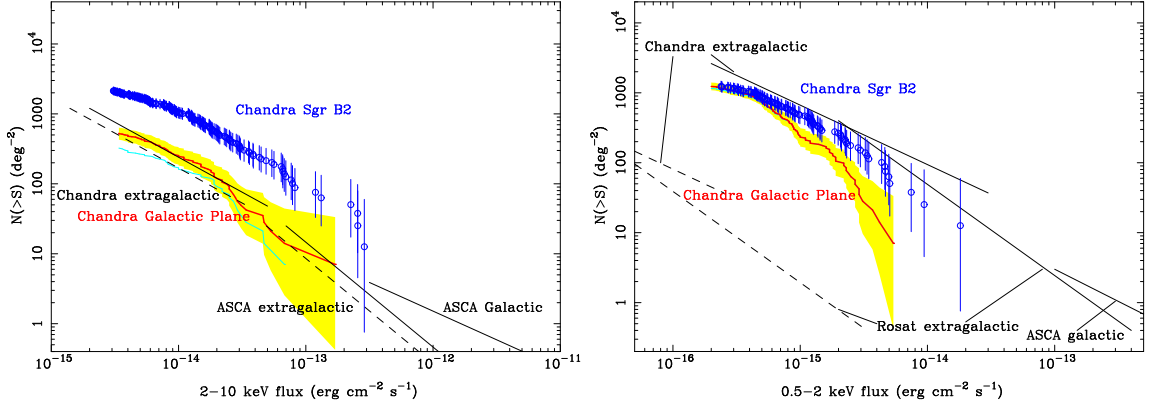


Figure 3. The $\log N - \log S$ curves of the point sources detected in our Chandra Galactic plane field in 2 – 10 keV (left) and 0.5 – 2 keV (right). They are indicated in red lines (in the electronic version) within the 90 % error regions (polygon shape in yellow). Together, other $\log N - \log S$ relations are shown for the bright ASCA Galactic sources (Sugizaki et al. 2001), Chandra Galactic center (Sgr B2) point sources and extragalactic point sources detected with ASCA (Ueda et al. 1999), ROSAT and Chandra (Giacconi et al. 2001). For the extragalactic sources, both the original $\log N - \log S$ curves at high Galactic latitudes and the ones expected on the Galactic plane with a hydrogen column density of $6 \times 10^{22} \text{ cm}^{-2}$ (broken lines) are shown. Also the $\log N - \log S$ curves of only the sources having the near infrared counterparts are shown in the left figure (slightly below our Chandra Galactic $\log N - \log S$ curve; cyan in the electronic version).

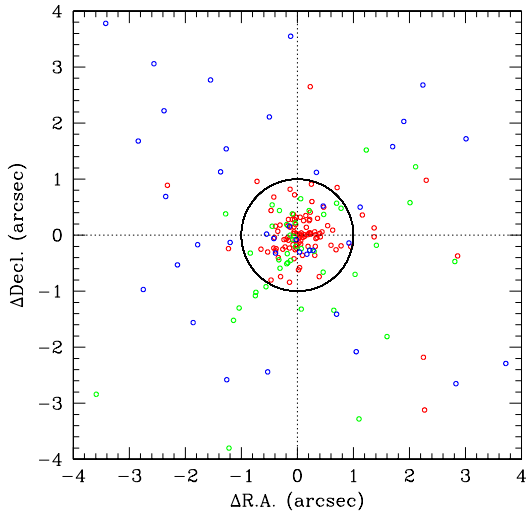


Figure 4. Distance between the Chandra point source and the nearest NIR source detected by SOFI. In the electronic version, soft, medium and hard X-ray sources are distinguished with red, green and blue, respectively.

sumably because they are intrinsically dim and/or very far Galactic sources. On the other hand, we can see that there are many *bright hard* sources which are not identified in NIR. In particular, the brightest Chandra source, which has the hardness ratio 0.74 (Fig. 5), is not identified in the NIR. This is not surprising since AGNs tend to be bright in hard X-rays, but even the brightest AGNs should be completely absorbed through the Galactic plane.

We have created composite (average) energy spectra of point sources, by dividing them into four cate-

gories, depending on the X-ray hardness (soft and hard) and presence or absence of the NIR counterparts (Fig. 6). The soft sources with NIR counterparts (top left) show thermal emission lines, and are fitted with the two-component thermal plasma model. This kind of spectrum is consistent with stellar coronal emission. The soft sources without NIR counterparts are dimmer but can be fitted with exactly the same model with decreasing normalization and increasing hydrogen column density, which suggests they are farther and/or dimmer active stars.

Hard X-ray sources with NIR counterparts, even though only handful, indicate a clear narrow iron emission line at 6.67 keV from helium-like ions and a flat continuum spectrum. This is a signature of a high temperature thermal plasma, expected from quiescent cataclysmic variables. On the other hand, the hard X-ray sources without NIR counterparts are *brighter*, and they show rather complex iron features which look like broad lines or edges. The X-ray brightness and complex iron feature supports the idea that these hard X-ray sources without NIR counterparts are background AGNs.

REFERENCES

- Bamba, A., Ueno, M., Koyama, K. Yamauchi, S. 2001, PASJ, 53, L21
- Ebisawa, K., Maeda, Y., Kaneda, H. and Yamauchi, S. 2001, Science, 293, 1633
- Ebisawa, K. et al. 2004, in preparation
- Giacconi, R. et al. 2001, ApJ, 551, 624
- Sugizaki, M. et al. 2001, ApJS, 134, 77
- Ueda, Y. et al. 1999, ApJ, 518, 656
- Ueno, M., Bamba, A., Koyama, K. and Ebisawa, K. 2003, ApJ, 588, 338

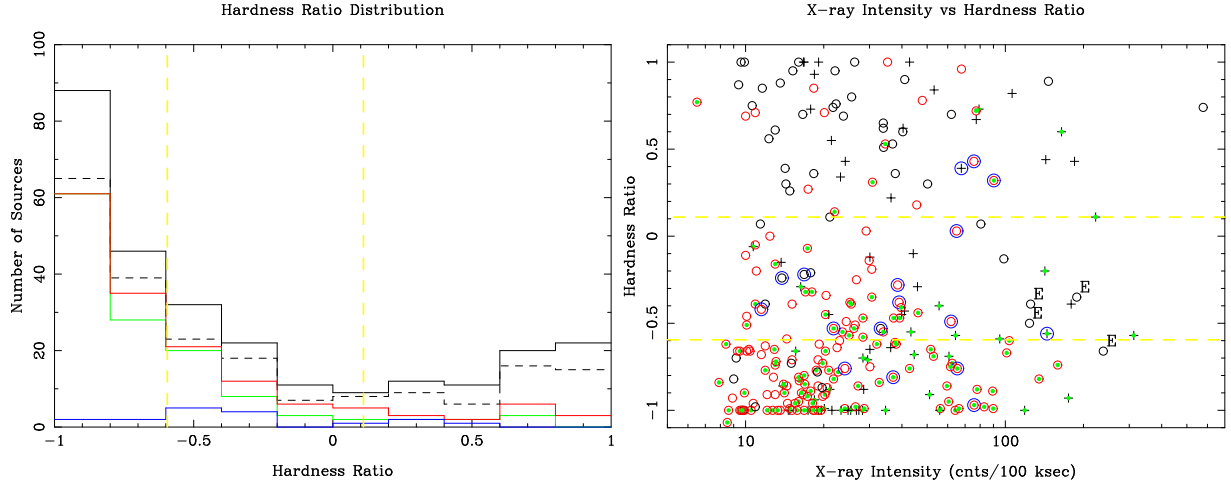


Figure 5. Histogram of the hardness ratio distribution (left) and intensity-hardness diagram (right). The hardness ratio is defined as $(H - S)/(H + S)$, where S and H are vignetting-corrected counting rates in $0.5 - 2$ keV and $3 - 8$ keV, respectively. In the left panel, the broken line indicates the number of sources within the SOFI fields, and the line below (red in the electronic version) shows the sources having the SOFI near-infrared counterparts. The green line (below red) tells the number of sources having the 2MASS counterparts, and the blue line (bottom) is for the variable sources. In the right panel, the sources outside of the SOFI field are shown with crosses, and those inside are with circles. In the electronic version, black circles indicate sources without SOFI counterparts, while red circles are those having the SOFI counterparts. In addition, sources having the 2MASS counterparts are marked with green dots, and variable sources are marked with blue circles. The horizontal broken lines (yellow) in both figures indicate the boundaries we defined between the soft and medium sources (hardness ratio=-0.595), and the medium and hard sources (hardness ratio=0.11).

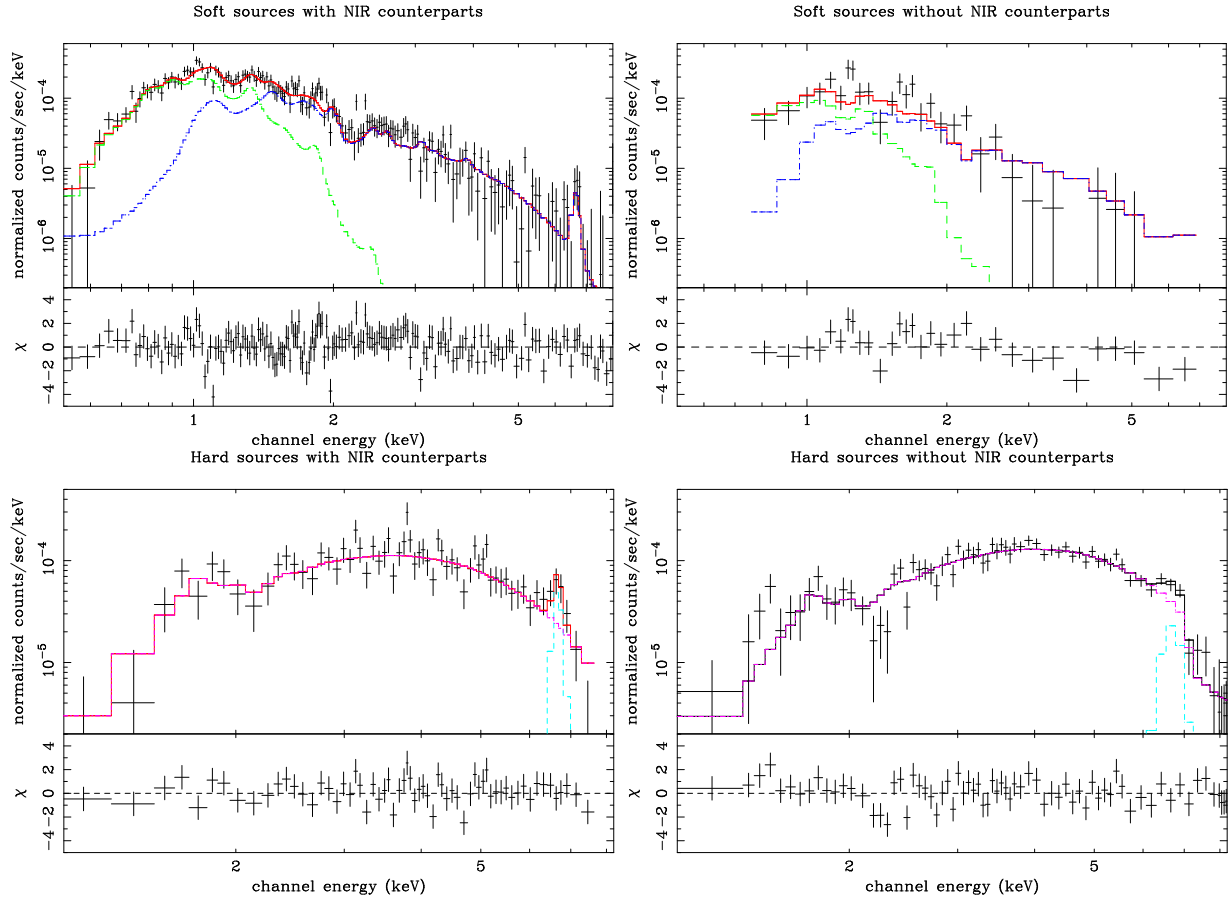


Figure 6. Composite energy spectra and model fitting of the point sources grouped by the X-ray spectral hardness and absence or presence of the NIR counterparts. Those having the NIR counterparts are in the left-hand side, and those without the NIR counterparts are in the right-hand side. The top two panels are the soft source spectra, and the bottom ones the hard source spectra.

